An improved Artificial Rabbit Optimization for structural damage identification

Quyet Nguyen Huu[a] (iD), Lan Nguyen Ngoc[b] (iD), Thanh Bui Tien[b] (iD), Hoa Tran Ngoc[b] (iD), Hieu Nguyen Tran[c] (iD), Tung Nguyen Xuan[d]* (iD)

[a]DX Laboratory, The University of Transportation and Communications Limited Company (UCT), Vietnam. Email: quyet.official@outlook.com

[b]The Department of Bridge Engineering & Underground Infrastructure, Faculty of Civil Engineering, University of Transport and Communications, Hanoi, Vietnam. Email: nngoclan@utc.edu.vn; btthanh@utc.edu.vn; ngochoa@utc.edu.vn

[c]Faculty of Information Technology, University of Transport and Communications, Hanoi, Vietnam. Email: nthieu@utc.edu.vn

[d]Structural Engineering Department, University of Transport and Communications, Hanoi, Vietnam. Email: ngxuantung@utc.edu.vn

* Corresponding author

Abstract

This paper presents an enhanced version of the Artificial Rabbit Optimization (ARO) algorithm designed for identifying structural damage in bridge structures. The original ARO draws inspiration from survival observed in wild rabbits. However, it demands a substantial investment of computational time. Therefore, in this paper, the Improved ARO (IARO) algorithm incorporating elements of the Grey Wolf Optimizer (GWO) through hybridization, is employed to deal with optimization problems. The central concept of this approach involves infusing predator-hunting characteristics into the prey-rabbit during the hunting process, thereby enabling more effective predator evasion. The proposed method is evaluated through a series of simulations related to two real bridges: a simple supported beam structure and a steel truss bridge. The results show a significant improvement in accuracy and efficiency in determining structural damage while considering factors such as damage location, severity, and computation time. These findings underscore the potential of the proposed approach for real-world applications in structural health monitoring and damage detection.

Keywords

Graphical Abstract

1 INTRODUCTION

Structural Health Monitoring (SHM) represents a stimulating field dedicated to the ongoing assessment of structural conditions in entities like bridges, buildings, and infrastructure, with the primary aim of guaranteeing their safety and dependability (Barreto et al., 2021; Jahangiri et al., 2016; Marques et al., 2018). In recent years, notable progress has been made in advancing SHM systems and technologies, driven by the growing imperative of infrastructure maintenance and safety. However, the field confronts various challenges, encompassing the amalgamation of diverse sensor technologies, streamlined data processing, and accurate interpretation of monitoring data. To surmount these challenges, methodologies, and technologies have been devised to process and analyze the extensive data amassed by SHM systems. The utilization of vibration sensors, which exhibits the capability to discern and quantify shifts in frequencies, thereby facilitating the discernment of structural damages. These sensors assume a pivotal role in capturing dynamic behaviors, thereby enabling the early detection of potential concerns, and facilitating proactive strategies for maintenance and repair. The combination of vibration characteristics, such as frequencies, mode shapes, and damping ratio, with other technologies as followed metaheuristic algorithms has shown great potential in the field of damage identification. Changes in these characteristics can indicate the presence of damage. Vibration-based damage identification relies on analyzing changes in the dynamic response of a structure to detect and locate damage (Das et al., 2016; Gordan et al., 2017; Ngoc-Nguyen et al., 2022; Rajenderan and Jayaguru, 2022).

Optimization algorithms offer significant benefits across a wide range of disciplines. They adeptly identify optimal or nearly optimal solutions through systematic exploration of search spaces, outperforming exhaustive search approaches. These algorithms can manage problems of varying magnitudes and intricacies, display adaptability across diverse domains and effectively address expansive optimization issues. They exhibit the capacity to flexibly modify strategies, operators, and parameters to accommodate shifting problem dynamics, ensuring efficacy in practical scenarios. Notably versatile, optimization algorithms find application in multiple domains, serving as potent tools for intricate predicaments in engineering, logistics, finance, and machine learning. For example, (Yıldız et al., 2019) proposed the hybrid Harris Hawks-Nelder-Mead optimization (H-HHONM) for design and manufacturing problems. The results compared with some other algorithms showed that H-HHONM is an effective optimization approach for optimizing both design and manufacturing problems. In the research (Zhang et al., 2019), the authors used a colony optimization algorithm to find the route optimization problem. The findings indicated that decrease in the total logistics expenses and a reduction in carbon emissions. (Liu et al., 2013) introduced a new approach to solving processing plans by considering the machining constraints and goal of Ant Colony Optimization (ACO). The computational outcomes demonstrated that the ACO algorithm outperforms the other three algorithms including Tabu Search (TS), Simulated Annealing (SA), and Genetic Algorithm (GA). An optimization algorithm namely honey-bee mating used for resolving educational timetabling problems (Sabar et al., 2012). In certain instances, the proposed approach outperforms alternative methods, showcasing its potential as a promising solution.

By incorporating these parameters into the objective function of the metaheuristic algorithm, the algorithm searches for the optimal combination of damage locations and severities that best match the observed vibration data such as Particle Swarm Optimization (PSO) (Gökdağ and Yildiz, 2012; Kang et al., 2012; Nguyen-Ngoc et al., 2021); Teaching Learning Based Optimization (TLBO) (Ahmadi-Nedushan and Fathnejat, 2022; Shahrouzi and Sabzi, 2018); Slime Mould Algorithm (SMA) (Ngoc-Nguyen et al., 2023), Artificial Hummingbird Algorithm (AHA) (Ngoc et al., 2023); Marine Predator Algorithm (MPA);…Besides, many hybrid metaheuristic algorithms combined with neural networks (Hoàng Việt et al., 2023; Su Fen et al., 2023) have also been applied to fault diagnosis, Feedforward Neural Networks and Marine Predator Algorithm (MPAFNN) (Ho et al., 2021b); Grey Wolf Optimizer and Artificial Neural Networks (GWOANN) (Ho Viet et al., 2022); Particle Swarm Optimization-Gravitational Search Algorithm (PSOGSA); Feedforward Neural Network-Particle Swarm Optimization and Gravitational Search Algorithm (FNN-PSOGSA) (Ho et al., 2021a).

In recent years, a novel metaheuristic algorithm called Artificial Rabbit Optimization (ARO) has been successfully applied in numerous fields. This algorithm, introduced by Wang (Wang et al., 2022), draws inspiration from the inherent behaviors of rabbit species, encompassing their foraging tendencies and predator evasion strategies. ARO has been conducted by various researchers in their investigations. For instance, (Alsaiari et al., 2023) merged ARO with a multi-layer perceptrons (MLP) model to predict the water efficiency of different configurations of solar stills (SSs). Another study (Alamir et al., 2023) introduced a modified ARO approach, infused with principles from quantum mechanics, showcasing its efficacy in solving energy management (EM) problems by optimizing benefits and reducing time consumption. Furthermore, (Samal et al., 2023) effectively employed ARO to address economic load dispatch challenges. Despite the notable achievements highlighted in the aforementioned research, ARO does present certain limitations. Notably, it entails a relatively extensive computational timeframe and exhibits a moderate level of precision in its outcomes. Given the significant values of random coefficients within the algorithm, we propose a refinement to ARO in this study. This involves incorporating the foraging strategy from the Grey Wolf Optimizer (GWO) algorithm (Mirjalili et al., 2014), with the aim of enhancing outcomes during the computational phase of ARO.

Nevertheless, it is commonly acknowledged that this algorithm still contains fundamental shortcomings. First, the computational intricacies stemming from amalgamating multiple vibration traits with metaheuristic algorithms can prove substantial, particularly when dealing with extensive structures. Furthermore, the task of selecting optimal optimization parameters and performing a crucial objective function that effectively encapsulates the interplay between vibration characteristics and damage variables demands careful consideration and domain-specific expertise. Therefore, this study introduces an innovative avenue for resolving structural damage identification predicaments by harnessing an enhanced version of the ARO (IARO). This methodology is applied to tackle the damage identification concerns associated with the My Thanh 1 bridge and the Cua Rao truss bridge. Certainly, the study offers noteworthy contributions:

- Introduction of an enhanced optimization algorithm referred to as IARO. This advancement integrates the hunting tactics of grey wolves, consequently enhancing the balance between exploration and exploitation. This increase not only strengthens the algorithm's recovery capabilities but also minimizes the risk of getting stuck in local optimization.

- Demonstration of the efficiency and precision of the proposed approach via two compelling case studies. Firstly, the methodology is applied to a prevalent bridge type commonly found in the Southeastern provinces of Vietnam – the reinforced concrete girder bridge. Secondly, the efficacy of the developed algorithm is gauged through its application to a series of truss bridge scenarios. The practical assessment in these diverse scenarios underscores the method's effectiveness across varying structural contexts.

In sum, the study showcases a unique optimization technique, IARO, accentuating its advantages through very realistic case studies in distinct bridge types. The paper consists of four main sections: it begins by introducing the research problem and proposing the methodology. Section 2 presents the fundamentals of the ARO algorithm and its enhancement through the foraging strategy of the GWO. The applied subjects encompass two types of structures: simply supported reinforced concrete beams and steel truss bridges. The final section comprises the conclusion.

2 IMPROVED OPTIMIZATION ALGORITHM

2.1 Artificial Rabbit Optimization (ARO)

The ARO algorithm draws its inspiration from two survival tactics that wild rabbits employ. These strategies enhance the rabbits' chances of survival when confronted by predators. The first tactic involves the rabbits consuming grass near their nests, minimizing the risk of detection (Figure 1). The second strategy (Figure 2), termed "random hiding," entails relocating rabbits to various nearby burrows, thereby augmenting their concealment. The algorithm's mathematical interpretation is constructed in these two tactics, incorporating their principles in a complex manner. Additionally, a crucial factor of the algorithm involves the transition between exploration and exploitation modes, determined by the rabbit's energy degradation coefficient.

$$\vec{P}_x(t+1) = \vec{P}_y(t) + LR.MV.\left[\vec{P}_x(t) - \vec{P}_y(t)\right] + round\left(0,5 + (0,5 + c1).s_1\right) \tag{1}$$

$$x, y = 1 : nPop; x \neq y; s_1 \sim N(0,1)$$

$$LR = \left(e - e^{\left(\frac{t-1}{iteration}\right)^2}\right) \times \sin(2\pi c_2) \tag{2}$$

$$MV_{(z)} = \begin{cases} 1 \, if \, z = p(i) \\ 0 \, else \end{cases} z = 1,...,q; i = 1,...[c_3, q]; p = rand(q) \tag{3}$$

In which $\vec{P}_x(t+1)$: new-updated position of the artificial rabbit at the time $(t+1)$, $\vec{P}_y(t)$ is the old location of the xth rabbit at the time t; $nPop$: Total population number of artificial rabbits, q: variable numbers of the problem, and $Iteration$: the maximum number of iterations considered. LR: the length the rabbit has run during the deviation feeding with MV is a mapping vector; c_1, c_2: random parameters between $[0,1]$, s_1: standard normal distribution.
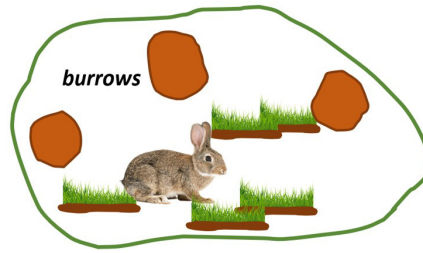
Figure 1 Exploration
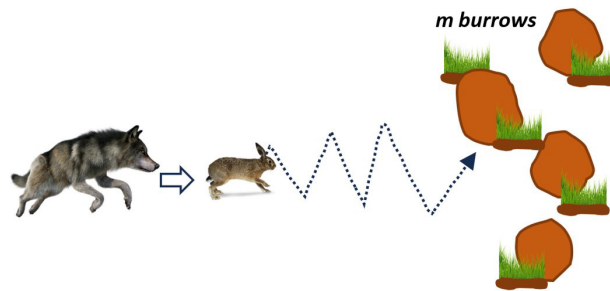
Figure 2 Exploitation

Within their safe environment, rabbits utilize deceptive strategies by constructing imitation burrows that resemble their genuine burrow. They employ a random selection process to determine their hiding location, further enhancing their survival prospects against various predators. The formulation of this process, where the xth rabbit creates the yth burrow, is expressed as equation (4):

$$\overrightarrow{BR_{x,y}}(t) = \overrightarrow{P_x}(t) + h.p.\overrightarrow{P_x}(t), x = 1,...,nPop; \ y = 1,...,m \tag{4}$$

$$p(P) = \begin{cases} 1 & if \quad P == p(i) \\ 0 & else \end{cases} \tag{5}$$

The concealment parameter is denoted as h, gradually decreases from 1 to $1/Iteration$ in a linear manner throughout the iteration process, incorporating random perturbations $\overrightarrow{BR}_{x,y}(t)$ represents a randomly chosen burrow for the rabbit to seek safety from danger among m burrows are created. The mathematical expression for the rabbit's random hiding behavior is indicated as equation (6) below:

$$\overrightarrow{P_x}(t+1) = \overrightarrow{P_x}(t) + LR.MV.\left(c_3 \times \overrightarrow{BR_{x,\alpha}}(t)\right) \tag{6}$$

$$\overrightarrow{BR_{x,\alpha}}(t) = \overrightarrow{P_x}(t) + h.\rho.\overrightarrow{P_x}(t) \tag{7}$$

The variable $\overrightarrow{BR}_{x,\alpha}(t)$ is the random selection of a burrow for the specific intent of finding a hiding spot. Following the successful completion of both the deviation feeding and c phase, the position of the xth rabbit is calculated using equation (8):

$$\overrightarrow{P_x}(t+1) = \begin{cases} \overrightarrow{P_x}(t) \underline{\quad\quad} f\left(\overrightarrow{P_x}(t)\right) \le f\left(\overrightarrow{P_x}(t+1)\right) \\ \overrightarrow{P_x}(t+1) \underline{\quad\quad} f\left(\overrightarrow{P_x}(t)\right) > f\left(\overrightarrow{P_x}(t+1)\right) \end{cases} \tag{8}$$

Energy degradation coefficient: the initial phases typically prioritize exploration, while the later stages focus more on exploitation. However, the ARO algorithm incorporates a search strategy inspired by the energy degradation coefficient observed in rabbits. As the energy of the rabbits gradually decreases over time, the algorithm simulates the shift from exploration to exploitation by introducing a coefficient E, which controls the transition:

$$E(t) = 4\left(1 - \frac{t}{T}\right)\ln\frac{1}{c_4}; c_4 \in [0;1] \tag{9}$$

2.2 Improved Artificial Rabbit Optimization (IARO)

Although ARO has demonstrated effectiveness in addressing mathematical and engineering optimization problems, it has certain limitations. One of these shortcomings is the potential to become trapped in a local minimum, resulting in less accurate optimization outcomes. To overcome this issue, this study proposes an enhanced ARO algorithm by incorporating the hunting instinct of grey wolves from GWO to regulate the exploration or exploitation switch of ARO. In the original algorithm, the switch is determined by the energy degradation coefficient representing the loss of energy of the rabbit over time and indicates a transition from foraging to hiding for the rabbit. However, this approach may lead to the early-stage omission of global optima. In the proposed IARO, a new switching mechanism (Figure 3) is introduced based on the predatory behavior of grey wolves. In the wild, wolves circulate their prey until they are within a certain proximity for an attack. This instinct is applied to the artificial rabbit, enabling it to recognize predators within a specific radius, denoted as U. As long as the distance between the rabbit and the predator remains larger than this defined radius, the rabbit considers itself safe and continues foraging.
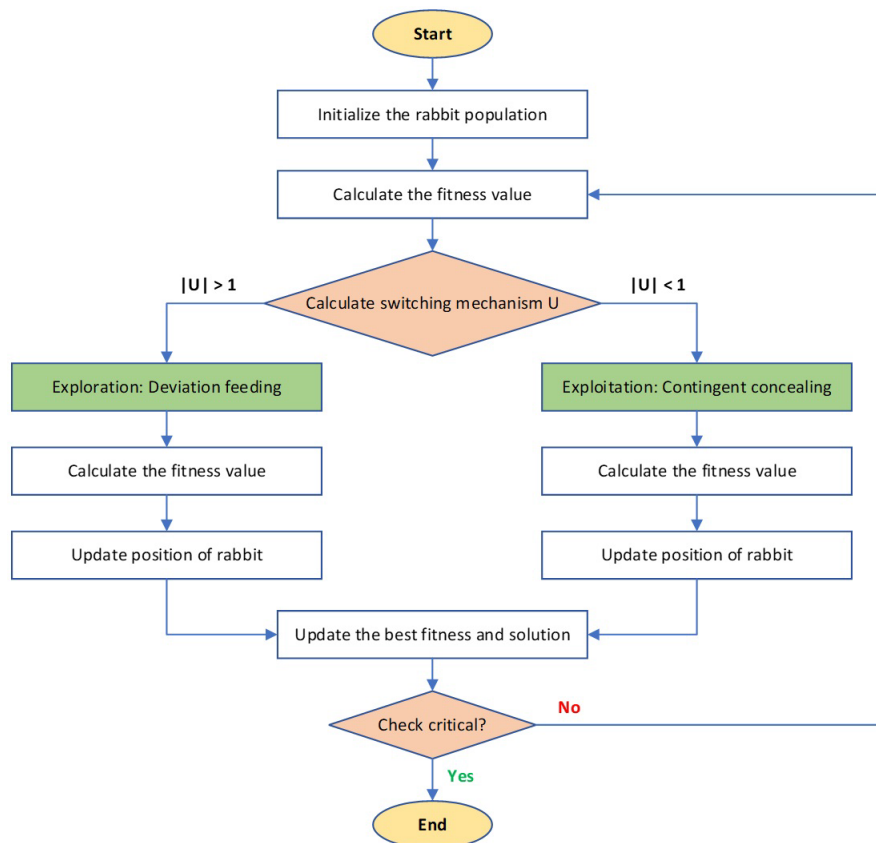
Figure 3 Flowchart of IARO algorithm

However, once the predator approaches closer than the defined threshold, the rabbit becomes alert and initiates random hiding. This switching mechanism (Figure 4) is mathematically expressed in equation (11) below:

$$\vec{U}(t) = 2 \times \vec{\theta} \times c_5 - \vec{\theta} \tag{10}$$

In which, c_5 is a stochastic variable in the range $[0,1]$, $\vec{\theta}$ represents a parameter subject to gradual reduction from an initial value of 2 to a terminal value of 0. The application of these parameters in equation (10) contributes to a diversification of update strategies. It achieves this by implementing the algorithm with dynamic characteristics, thereby averting entrapment in local optima during the exploration phase. Moreover, it optimizes the precision of algorithmic convergence and enhances the adaptability of the stochastic concealment phase.

$$Behaviour = \begin{cases} Exploration : Deviation\ feeding\ if\ |U| > 1 \\ Exploitation : Contingent\ concealing\ if\ |U| < 1 \end{cases} \tag{11}$$
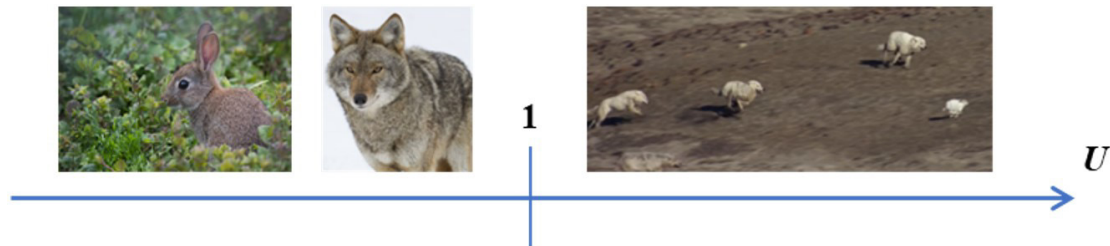
Figure 4 Switching mechanism

3 STRUCTURAL DAMAGE DETECTION USING IARO

3.1 Case study 1 – a supported simple beam bridge

In the first case study, My Thanh 1 bridge (Figure 5) is used for damage identification. The bridge is located at Km1526+033, QL1 in Ninh Thuan province, Vietnam, and consists of two lanes with a width of 11,0m. The main structure uses the simple reinforced-concrete inverse T-beam (Figure 6) with a length is 12m. Some components of the bridge such as abutments and parapets are built of concrete. In the southern regions of Vietnam, this type of bridge structure is frequently employed due to its simplicity in construction, quick implementation, coordinated production, and suitability for the local terrain, machinery, and cost considerations. More specifically, it is utilized for traversing areas where canals, creeks, small rivers, and streams are situated.

Figure 5 My Thanh 1 bridge (Ninh Thuan province)
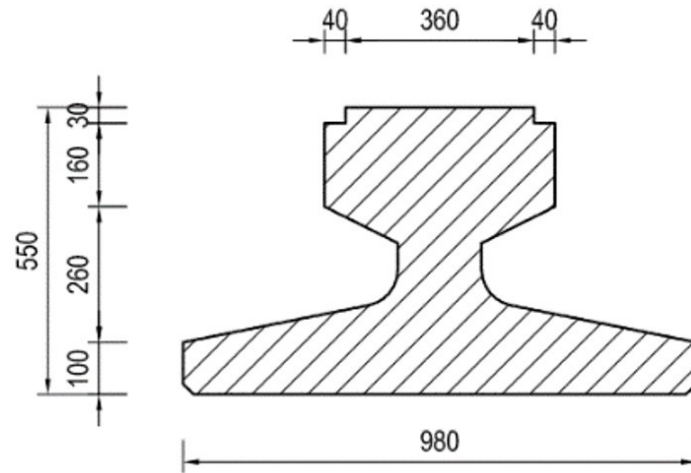
Figure 6 Cross section of the beam

By using the Stabil toolbox (François et al., 2021) that runs on the MATLAB program platform, a Finite Element Model (FE) of the bridge was created for dynamic characteristic analysis of the structure. The FE model consists of 25 nodes (24 nodes of structures, 1 reference node – Node 50) and 23 elements (Figure 7). The boundary conditions of the bridge include one fix bearing and one movable bearing. Geometric and material properties of beam elements are used in (Ngoc et al., 2023).
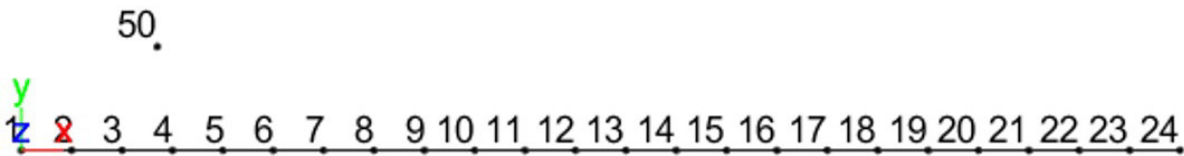
Figure 7 FE model of My Thanh 1 bridge

Two damaged cases have been assumed to evaluate the feasibility and effectiveness of the proposed algorithm IARO, attributed to the decrease in stiffness of the considered damaged element: single damage case and multiple damage case. In a single damage scenario (C1-1), the elastic modulus of only one element number 12 decreases by 23.7% of its original stiffness. In multiple damages scenario (C1-2), simulating multiple damaged elements case: the elastic modulus of elements number 12, 14, and 16 are reduced to 23.7%, 36.9%, and 30.1% of the original values respectively. The objective function is used to solve the problem as shown in equation (12):

$$ObjFcn = \sum_{t=1}^{n} \left\{ \frac{\left(f_{FEM} - f_d\right)^2}{\left(f_d\right)^2} + \left[1 - \frac{\left(\varphi_d^T \times \varphi_{FEM}\right)^2}{\left(\varphi_d^T \times \varphi_d\right)\left(\varphi_{FEM}^T \times \varphi_{FEM}\right)} \right] \right\} \tag{12}$$

In which n is the number of frequencies and corresponding mode shapes; f_{FEM} and φ_{FEM} are the frequencies and positions of the nodes in mode shapes to determine the damage; f_d and φ_d are the frequencies and positions of the nodes in mode shapes of the damaged structure; The symbol T represents the transpose matrix. The results are compared with the original algorithms of ARO using the same input parameters as the population of $nP = 1000$ and maximum iterations $MaxIt = 100$. Below are the outcomes obtained after executing the algorithm for each hypothetical scenario.

a) C1-1

b) C1-2
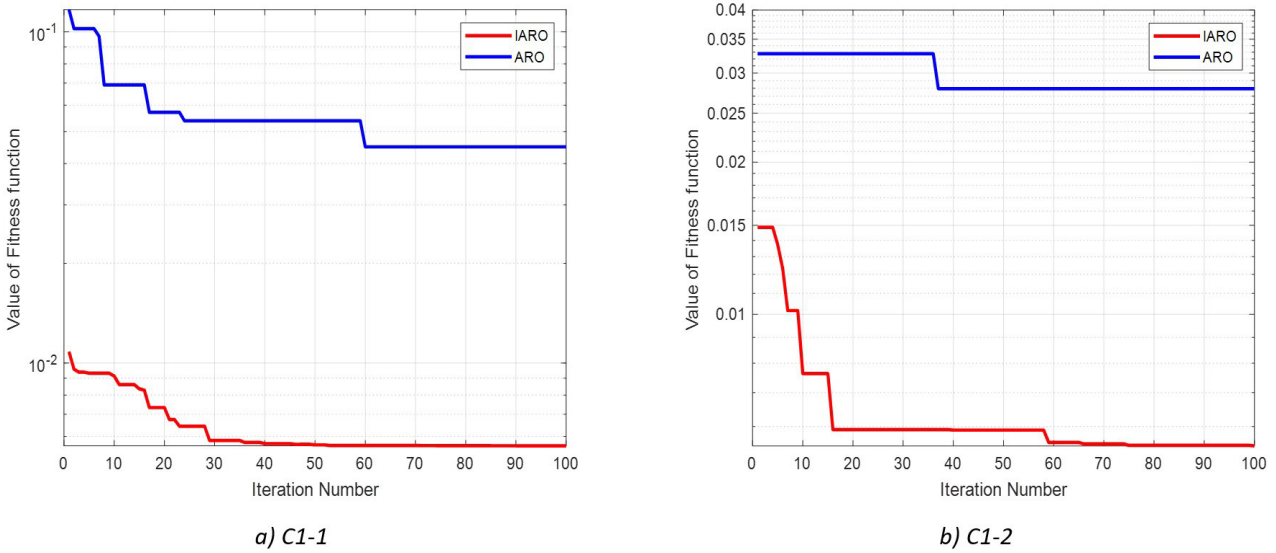
Figure 8 Best fitness so far in case study 1 (1)

Based on the outcomes presented in Figure 8 after 100 iterations, a distinct trend emerges. In both scenarios, the convergence performance of the ARO algorithm exhibits relatively modest progress, with minimal observable variations. Conversely, for the IARO approach, there is a considerable result. The best fitness value for IARO demonstrates a tendency to gradually decrease and approach proximity to the optimal value within the initial 30 iterations. Subsequently, this value stabilizes as the iterations progress towards completion.
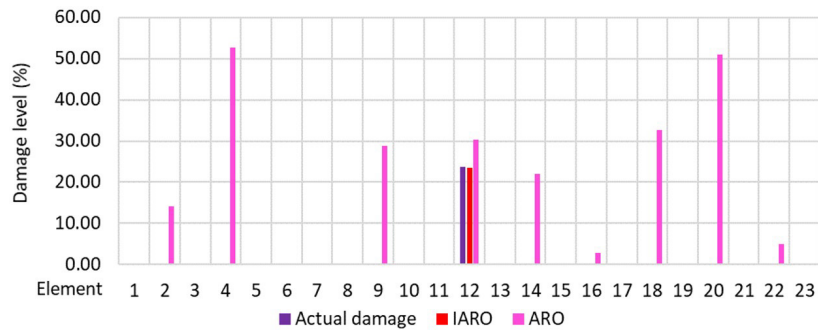
Figure 9 Location and damage level of C1-1

Analyzing the outcomes illustrated in Figure 9 for scenario C1-1, a distinct contrast becomes evident between the performance of IARO and ARO. Notably, the IARO algorithm stands out with superior results, successfully pinpointing the precise location of damage at element 12. Impressively, it accomplishes this with a minimal error rate of just 1,041%. On the other hand, ARO's performance falls short in comparison, exhibiting less accurate determinations for various damage locations. Most notably, the error recorded at the presumed damaged element reaches a substantial 28,189%.
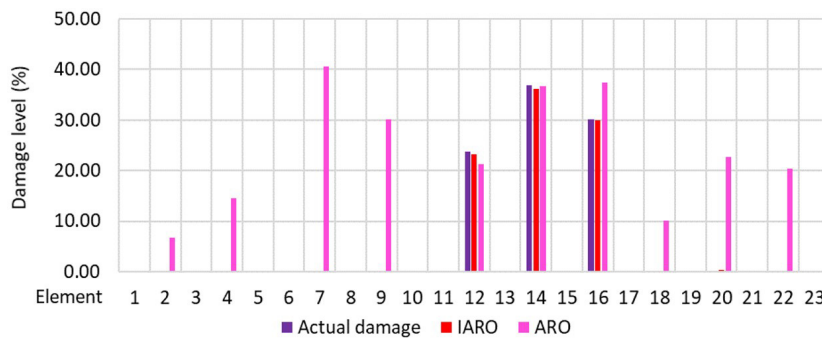
Figure 10 Location and damage level of C1-2

Reviewing the outcomes garnered from the scenario involving multiple damaged elements, IARO continues to shine with remarkable efficacy in precisely pinpointing both the location and extent of damage. Even at its maximum calculated error rate, which reaches 2,034%, IARO's performance remains commendable. Noticeably, this error occurs at element position 12, as depicted in Figure 10. Conversely, ARO persists in yielding inaccurate results, struggling to exactly identify the correct damage location and severity, further emphasizing the advantage of IARO's superior performance.

a) C1-1

b) C1-2
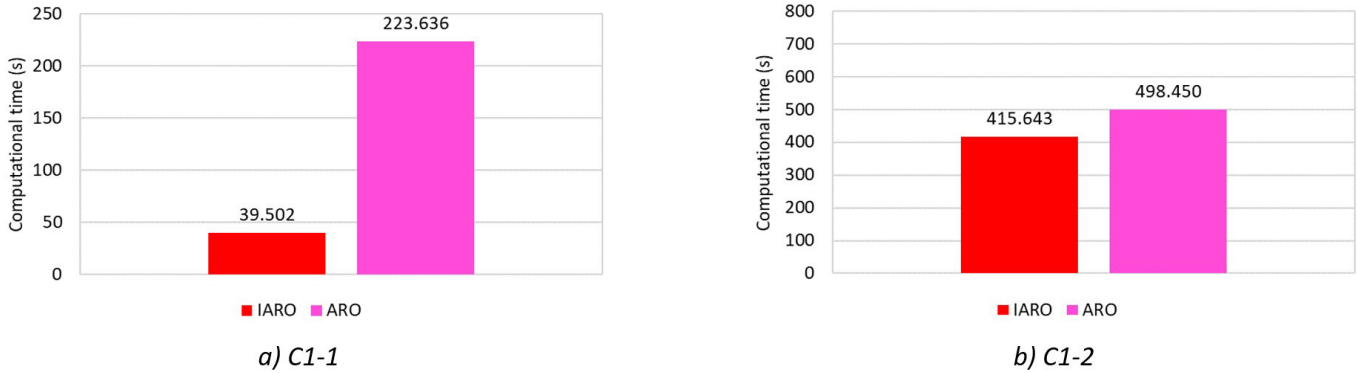
Figure 11 Computational time

Turning attention to the assessment of calculation time, as elucidated in Figure 11, an interesting trend appears across both scenarios. In both instances, IARO requires the shortest calculation time, demonstrating swiftness without compromising accuracy. Furthermore, the IARO algorithm consistently delivers precise outcomes pertaining to damage location and assessment, further solidifying its position as an efficient and effective solution in these scenarios.

In assessing the efficacy of the algorithm in damage detection problem, we examine positions analogous to those in cases C1-1 and C1-2 within smaller levels. Notably, for a structural configuration exhibiting singular damage (C1-3), The decrease in elastic modulus is recorded at 7.6%. Furthermore, in instances of multiple damages within the structure (C1-4), the residual stiffness values of individual elements are delineated as 92.4%, 95.2%, and 93.7%, respectively.

a) C1-3

b) C1-4
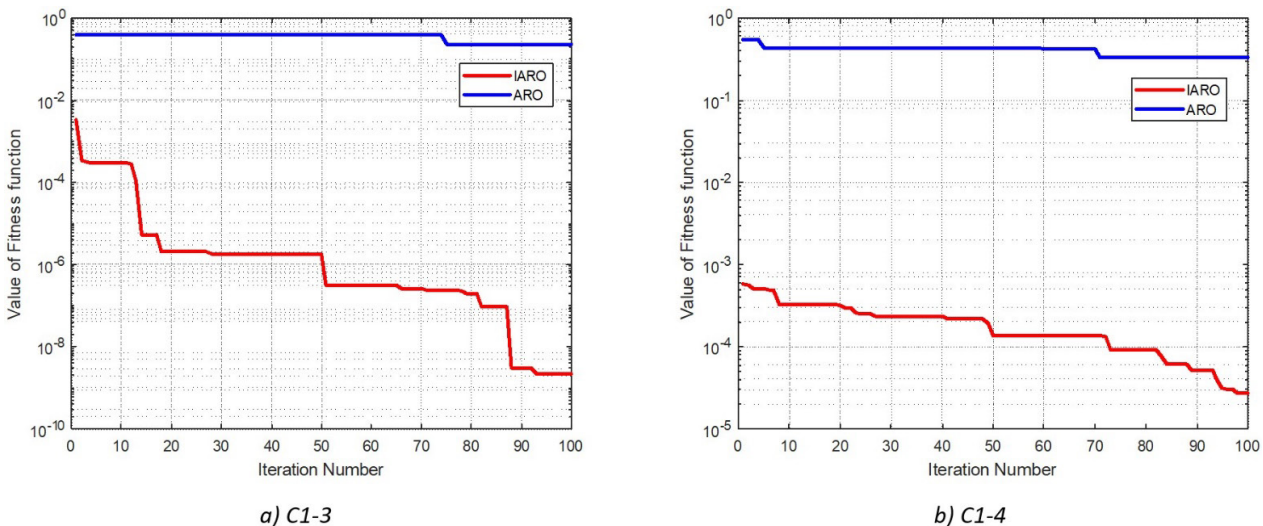
Figure 12 Best fitness so far in case study 1 (2)

Examining Figure 12's convergence chart reveals that the ARO algorithm's convergence values exhibit minimal changes across 100 iterations. In stark contrast, the proposed algorithm demonstrates a noteworthy trend of consistently decreasing toward value of fitness function, surpassing the performance of the original algorithm.
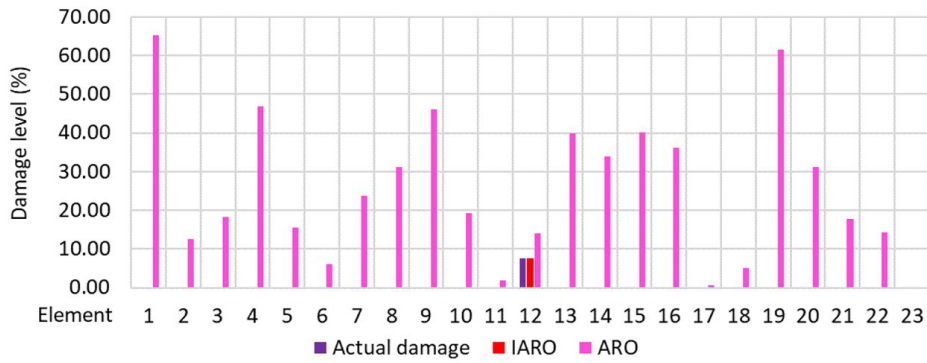
Figure 13 Location and damage level of C1-3
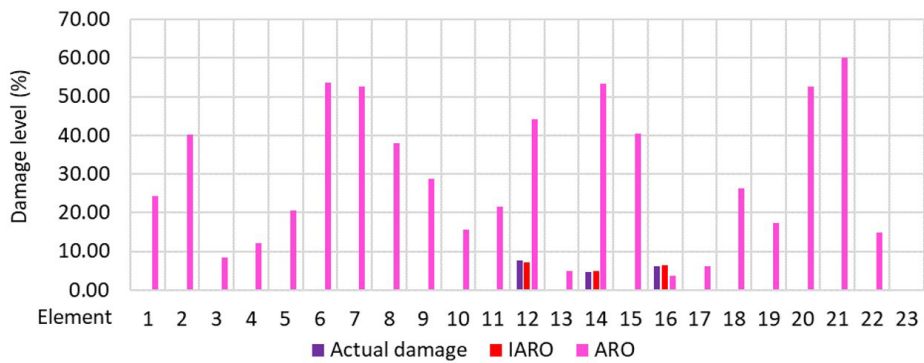
Figure 14 Location and damage level of C1-4

The outcomes depicted in Figure 13 and Figure 14 show that even when confronted with damage levels below 10%, the proposed algorithm consistently excels in accurately identifying damage locations across both scenarios. Specifically, the calculated error level in case C1-3 is only 0.201%, demonstrating the algorithm's precision. Meanwhile, in case C1-4, the largest error registers at 5.179% for element 14, while the smallest error is 0.898% for element 16. This imperfect identification is attributed to the algorithm's tendency to prioritize uniform determination of damage levels across elements, especially in structures with multiple damaged locations. Furthermore, it's important to note that the constrained number of iterations can also effect on the obtained results.

a) C1-3

b) C1-4
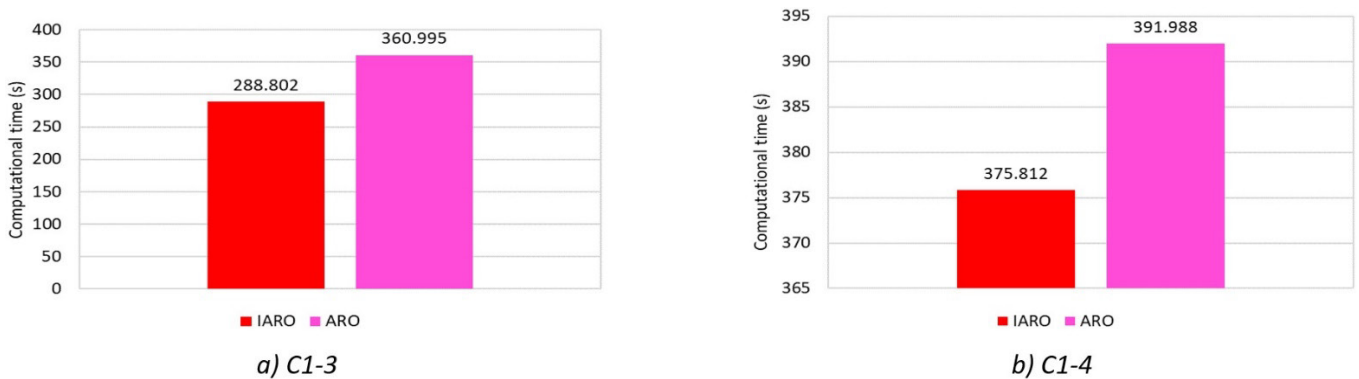
Figure 15 Computational time

The computation time (Figure 15) further indicates the efficiency and rapidity of the proposed algorithm, revealing a 4% decrease compared to the ARO algorithm in case C1-3 and an impressive reduction (about 20%) in case C1-4.

To consider the effect of the case of smaller stiffness reduction in different positions, such as near the bearings, we have also included the case of stiffness reduction of about 10%. The results are shown in Figure 16 - Figure 19.

- The structure has only 1 damaged element (C1-5): Element 1 reduces by 10%.

- The structure has 3 damaged elements (C1-6): Elements 1,2 and 3 reduced by 10%, 11% and 9% respectively.

a) C1-5

b) C1-6
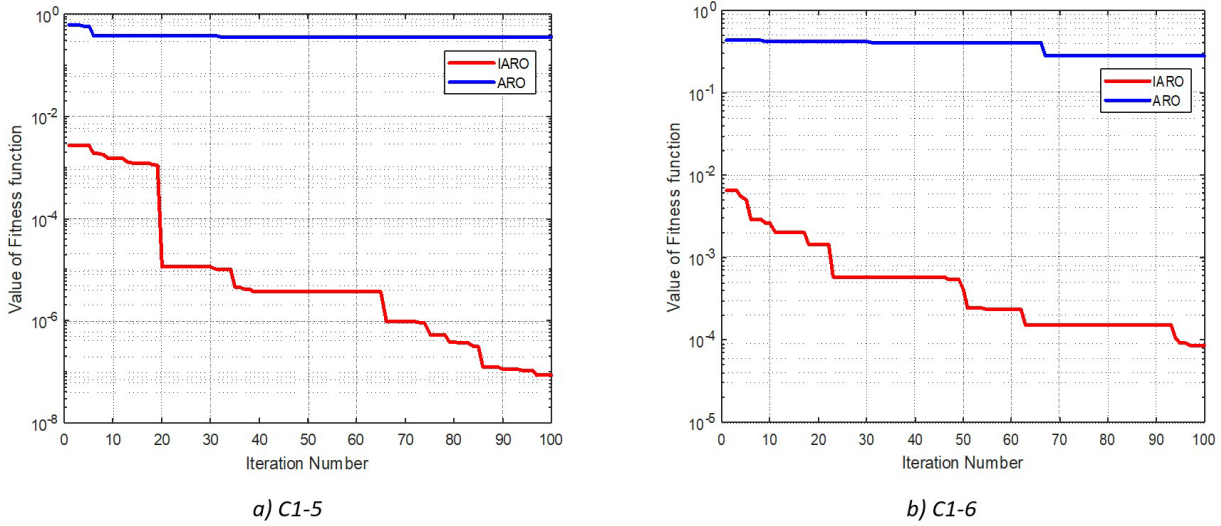
Figure 16 Best fitness so far in case study 1 (3)
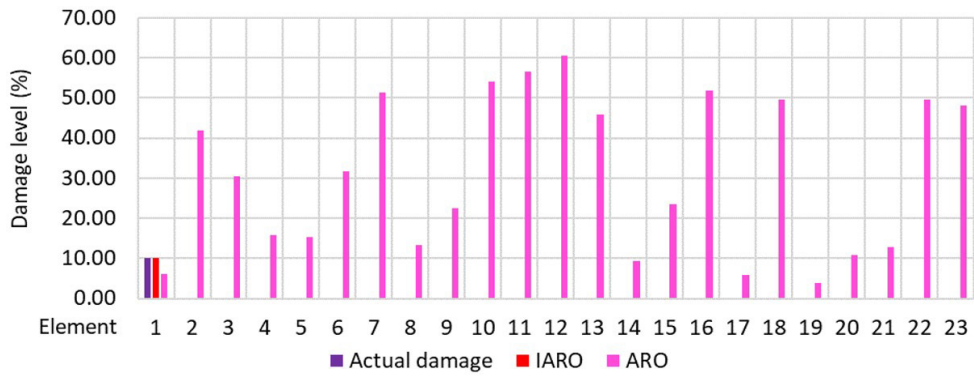
Figure 17 Location and damage level of C1-5
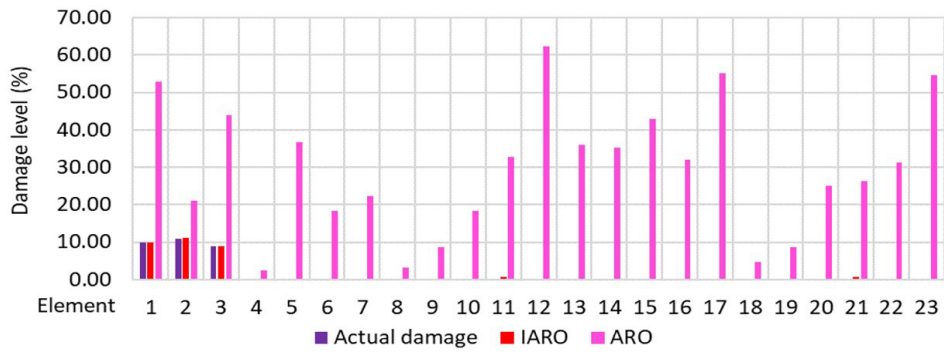
Figure 18 Location and damage level of C1-6

a) C1-5

b) C1-6
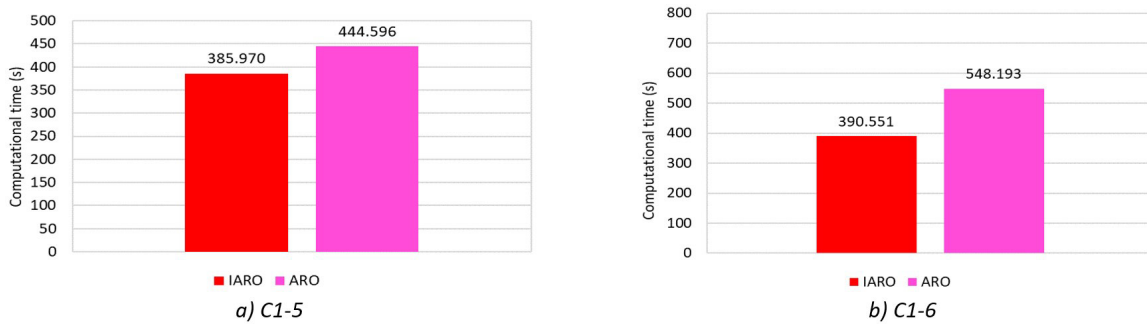
Figure 19 Computational time

Figure 16 to Figure 19 show a similarity of the results obtained in the previous four cases, particularly evident in the results for cases C1-5 and C1-6. Significantly, the proposed algorithm exhibits a convergence starting at a relatively low point and undergoes a substantial reduction within 100 iterations when compared to the original algorithm. This value signifies a low error in the objective function, reflecting a high degree of detecting accuracy. Furthermore, IARO accurately identifies damaged locations located closer to the supports, with the largest error for both cases not exceeding 1.939%. In terms of computation time, the proposed algorithm maintains its efficiency, demonstrating a faster processing speed.

3.2. Case study 2 – a truss bridge

Cua Rao Bridge depicted in Figure 20 is a steel warren bridge purposed for railway transportation. It is situated at the Km360+450 mark on the North-South railway line in Vietnam. Given its intricate location and the need for rapid completion, the construction technique employed was prefabrication (Figure 21). The project to build the bridge began in 2012 and encompasses these structural elements: two basic steel truss spans, each spanning 66.4 meters, and one simple steel beam span measuring 34 meters in length.

Figure 20 Cua Rao bridge

Figure 21 Sensors used for measurements

The initial finite element model (Figure 22) of a truss span is constructed with 53 truss joints and 143 elements representing the structural components. The geometric characteristics of these elements were computed based on field measurements of practical dimensions. The boundary conditions of the model were simulated using bearing supports. Additionally, due to the exclusive use of steel as the primary material throughout the beam, material parameters such as the elastic modulus $E = 2.00 \times 10^{11}\ N/mm^2$, Poisson's ratio $\mu = 0.3$, and density $W = 7850 kg/m^3$ were used. Following on-site measurement results, the updating of parameters including the elastic modulus of individual elements and the stiffness of the bearings was executed. Ultimately, a model closely resembling reality was obtained.
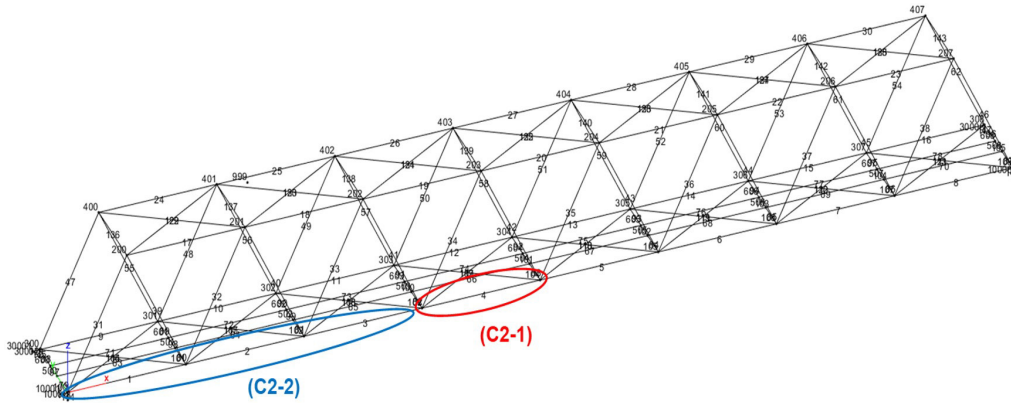
Figure 22 FE model of Cua Rao bridge

Assuming scenarios of damage with an update model similar to the case study 1 for 16 elements in the bottom chord components, for the case of the bridge structure where only one element is damaged (C2-1), the elastic modulus of element number 4 is reduced by 28.36%. In situations where multiple damaged elements appear within the structure (C2-2), the elastic modulus of elements number 1, 2, and 3 decrease by 33.55%, 30.48%, and 28.36% respectively. The objective function used for case study 2 is like case study 1 and is shown in equation (12). Given the increased complexity of the structure compared to Case study 1, to achieve meaningful results and ensure effective comparisons, the input parameters for algorithm execution are set as follows: a population size of $nP = 300$ and a maximum of 200 iterations.

a) C2-1   *b) C2-2*
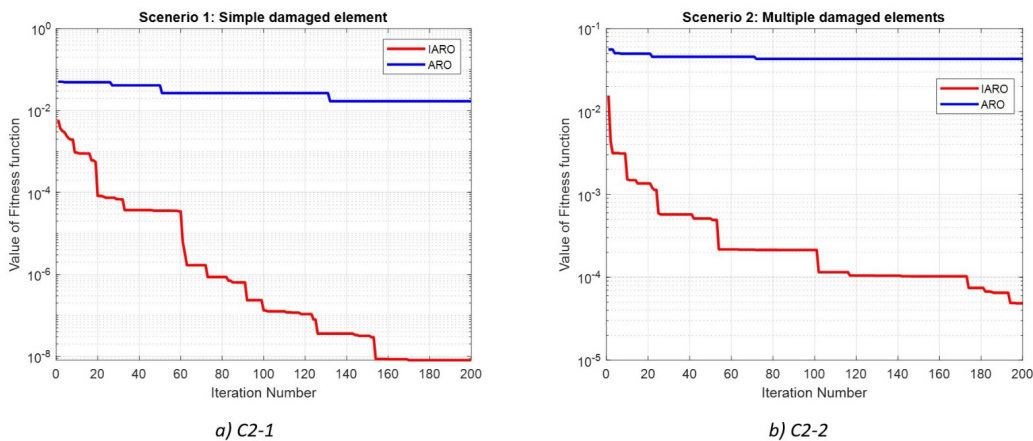
Figure 23 Best fitness so far in case study 2 (1)

The convergence values obtained from Figure 23 serve to highlight a positive outcome: within the context of the more complicated structural configuration explored in case study 2, the IARO method still consistently exhibits a notably superior convergence rate as compared to the ARO approach. Remarkably, the convergence speed and value of the ARO approach remain almost constant throughout the entirety of the process. In the C2-1 case, convergence is effectively achieved by the 150th iteration, and this state of convergence is sustained until the computation reaches its objective function. Conversely, in the C2-2 scenario, convergence stabilizes, even though there exists the potential for enhanced results through a higher iteration count. Nonetheless, the predetermined iteration count within this configuration effectively ensures precise diagnostic results.
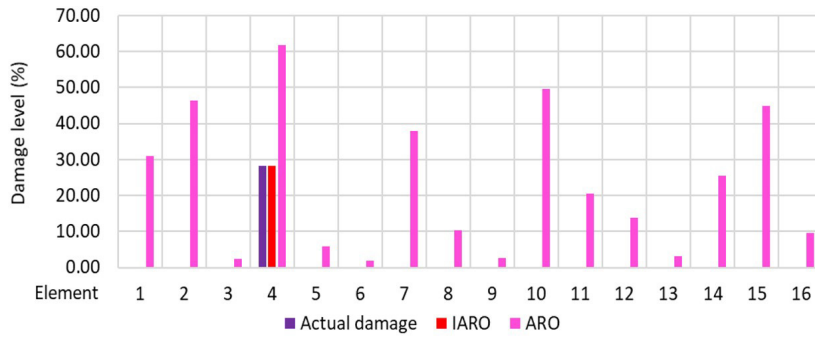
Figure 24 Location and damage level of C2-1
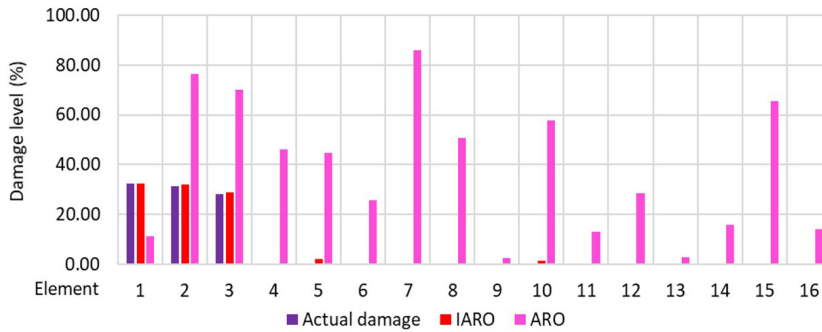
Figure 25 Location and damage level of C2-2

In Figure 24 and Figure 25, it becomes evident that the outcomes generated by the ARO algorithm are marked by a notable deficiency in accurately discerning the locations of damaged components. Additionally, the extent of damage is not accurately assessed. Significantly, this discrepancy is more pronounced in complex structural configurations characterized by a multitude of elements exhibiting diverse attributes. On the contrary, the IARO algorithm exhibits remarkable efficacy, particularly in scenarios involving intricate structural types. In these cases, the IARO algorithm successfully pinpoints the precise locations of damage, all the while maintaining a degree of damage assessment error of less than 2%. This robust performance underscores the IARO algorithm's ability to excel, especially when dealing with the challenges posed by complex structural configurations.

a) C2-1

b) C2-2
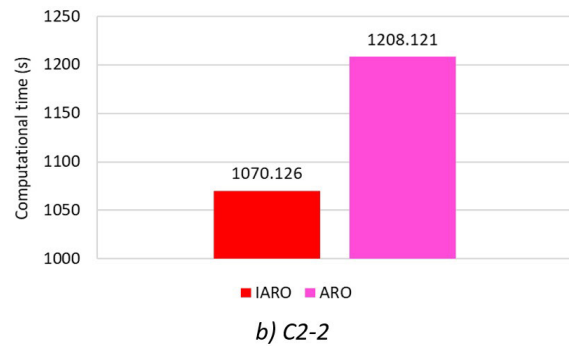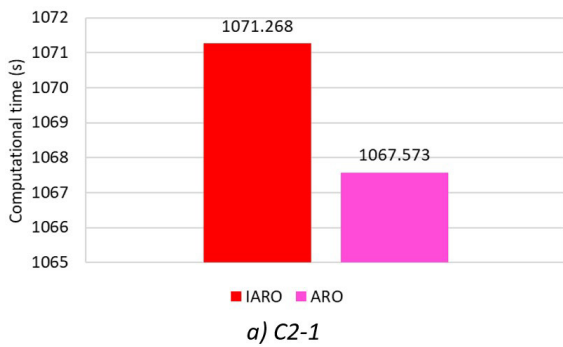
Figure 26 Computational time

Analyzing case C2-1 as depicted in Figure 26, it's apparent that both algorithms required around 1070 seconds to reach convergence. However, a distinct distinction emerges in the case of C2-2. Here, the IARO algorithm accomplishes both the identification of damage location and extent within the same timeframe of approximately 1070 seconds. In contrast, the ARO algorithm not only demanded a lengthier computation period to conclude the process but also produced imprecise outcomes. This disparity in both efficiency and accuracy reinforces the superiority of the IARO approach, especially when contrasted against the limitations of the ARO algorithm.

As the first case, to consider the effect of the case of smaller stiffness reduction for elements are closer to the supports, we have also included the case of stiffness reduction of about 10%. The results are shown below.

- The bridge has only 1 damaged element (C2-3): Element 1 reduces by 10%.
- The bridge has 3 damaged elements (C2-4): Elements 1,2 and 3 reduced by 10,11 and 9% respectively.

a) C2-3   b) C2-4
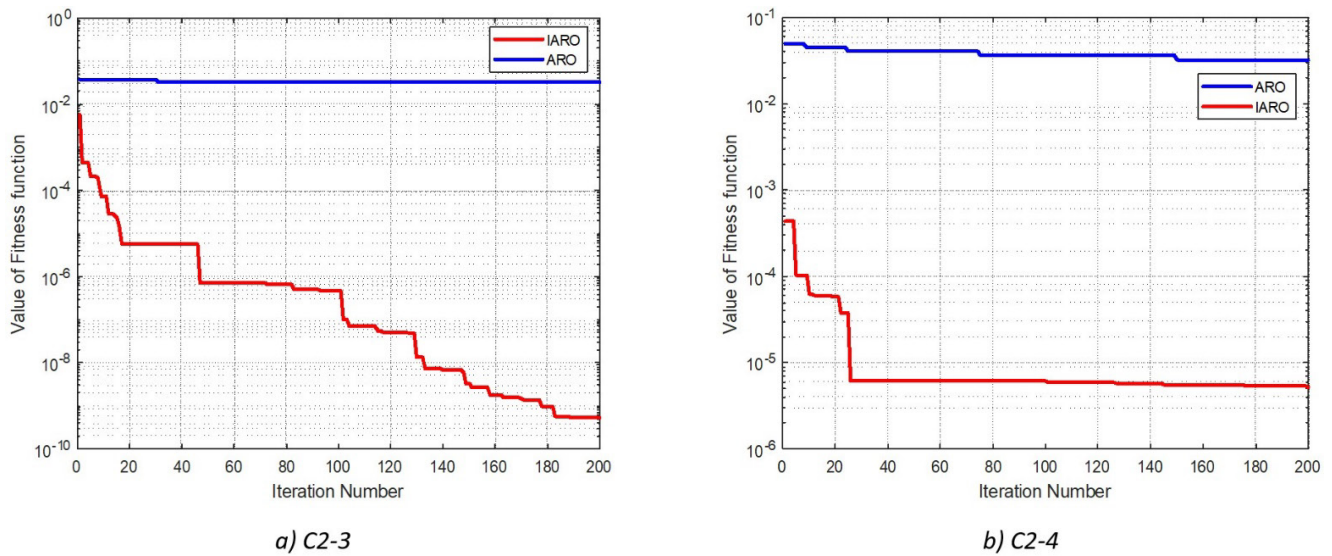
Figure 27 Best fitness so far in case study 2 (2)

Looking at the convergence chart in Figure 27 shows that the ARO algorithm's convergence values change mildly over 200 iterations. In contrast, the proposed algorithm shows a clear trend of steadily decreasing toward the fitness function value, performing better than the original ARO algorithm.
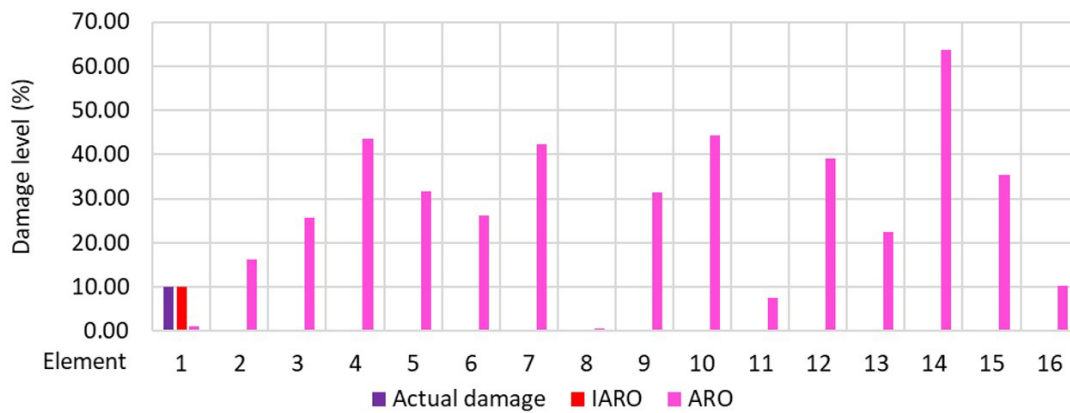
Figure 28 Location and damage level of C2-3
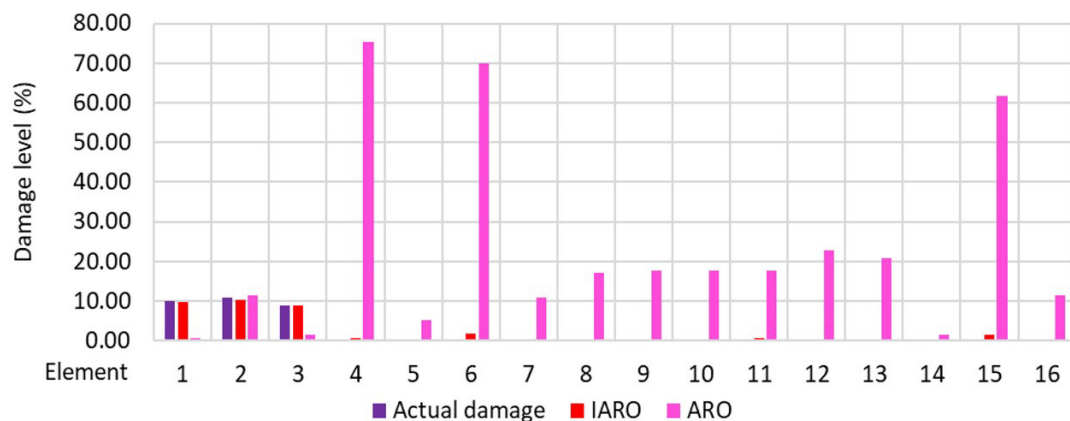
Figure 29 Location and damage level of C2-4

Even at its maximum calculated error rate of 5.679%, IARO's performance remains impressive. This error occurs at element position 2, as shown in Figure 28. Reviewing the outcomes from the situation involving three damaged elements in Figure 29, the IARO algorithm continues to perform remarkably well in accurately pinpointing both the location and extent of damage. On the other hand, the ARO algorithm continues to produce inaccurate results, struggling to correctly identify the damage location and severity. This further emphasizes IARO's superior performance with maximum error in detecting the damaged element is only 0.039%.

a) C2-3

b) C2-4
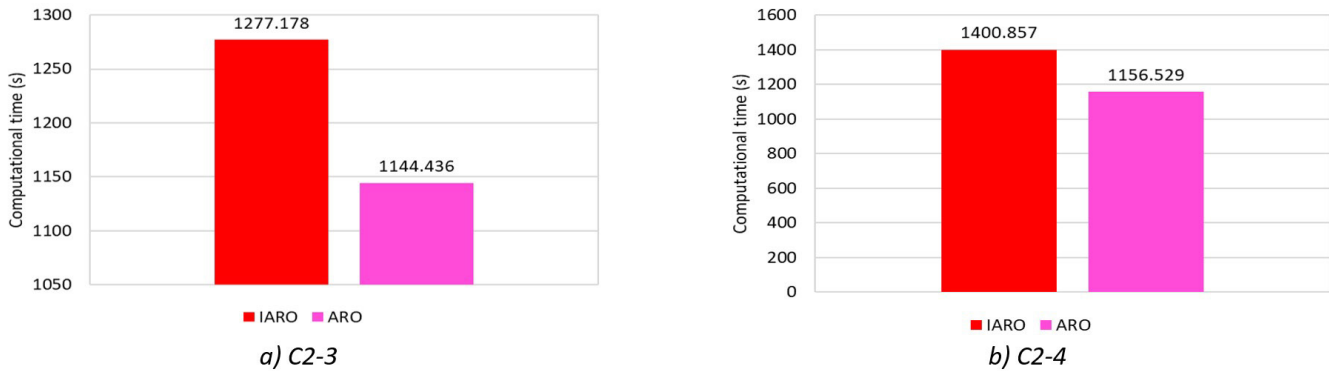
Figure 30 Computational time

Examining the chart presented in Figure 30, it is evident that the proposed algorithm requires a longer duration than the original algorithm to finalize the diagnosis process. In C2-3, this time difference amounts to 11.6%, while in case C2-4, it reaches approximately 21%. The primary factor contributing to this problem is attributed to the complex structure, random parameters, and the occurrence of the phase entering a local optimum from loop 25. Despite these challenges, the proposed algorithm maintains precision in assessing the stiffness reduction level of the element under the assumption of an initial condition.

4 CONCLUSIONS

This study undertakes a comprehensive evaluation of IARO in addressing structural damage identification problems. The investigation encompasses two distinct structural configurations: a simple reinforced-concrete beam and a steel truss bridge. The primary objective is to ascertain the algorithm's efficacy in contrast with the original ARO algorithm. The outcomes of the evaluation underscore the superiority of IARO in comparison to ARO. IARO consistently excels in accurately pinpointing both the location and severity of damage across single and multiple damage scenarios. The maximum error rate observed stands at only 2.03% in case study 1 and 1.64% in case study 2. Additionally, IARO achieves this heightened performance while significantly minimizing computational costs when compared to primary algorithms, all while maintaining a competitive convergence speed. These findings corroborate the prowess of IARO in optimizing structural damage identification processes. Importantly, IARO demonstrates its potential to enhance the current landscape of SHM systems, positioning it as a valuable tool for advancing structural integrity assessment.

Author's Contributions: Conceptualization, methodology, investigation, Quyet Nguyen-Huu and Lan Nguyen-Ngoc. Experiment, resources, software, writing – original draft, Quyet Nguyen-Huu. Writing - review & editing, Hoa Tran-Ngoc. Funding acquisition, Hieu Nguyen-Tran and Tung Nguyen-Xuan. Supervision, Thanh Bui-Tien.
Computer configuration: 12th Intel® Core™ i7-12700F 32GB RAM, NVIDIA GeForce 3060 RTX.

Editor: Pablo Andrés Muñoz Rojas

References

Ahmadi-Nedushan, B., Fathnejat, H., 2022. A modified teaching–learning optimization algorithm for structural damage detection using a novel damage index based on modal flexibility and strain energy under environmental variations. Engineering with Computers 38, 847–874. https://doi.org/10.1007/s00366-020-01197-3

Alamir, N., Kamel, S., Hassan, M.H., Abdelkader, S.M., 2023. An effective quantum artificial rabbits optimizer for energy management in microgrid considering demand response. Soft Comput. https://doi.org/10.1007/s00500-023-08814-5

Alsaiari, A.O., Moustafa, E.B., Alhumade, H., Abulkhair, H., Elsheikh, A., 2023. A coupled artificial neural network with artificial rabbits optimizer for predicting water productivity of different designs of solar stills. Advances in Engineering Software 175, 103315. https://doi.org/10.1016/j.advengsoft.2022.103315

Barreto, L., Machado, M., Santos, J.C., Moura, B.B.D., Khalij, L., 2021. Damage indices evaluation for one-dimensional guided wave-based structural health monitoring. Latin American Journal of Solids and Structures 18, 1-17. E354. https://doi.org/10.1590/1679-78256292

Das, S., Saha, P., Patro, S.K., 2016. Vibration-based damage detection techniques used for health monitoring of structures: a review. J Civil Struct Health Monit 6, 477–507. https://doi.org/10.1007/s13349-016-0168-5

François, S., Schevenels, M., Dooms, D., Jansen, M., Wambacq, J., Lombaert, G., Degrande, G., De Roeck, G., 2021. Stabil: An educational Matlab toolbox for static and dynamic structural analysis. Comput Appl Eng Educ 29, 1372–1389. https://doi.org/10.1002/cae.22391

Gökdağ, H., Yildiz, A.R., 2012. Structural Damage Detection Using Modal Parameters and Particle Swarm Optimization. Materials Testing 54, 416–420. https://doi.org/10.3139/120.110346

Gordan, M., Razak, H.A., Ismail, Z., Ghaedi, K., 2017. Recent developments in damage identification of structures using data mining. Latin American Journal of Solids and Structures 14, 2373–2401.

Ho, L.V., Nguyen, D.H., De Roeck, G., Bui-Tien, T., Wahab, M.A., 2021a. Damage detection in steel plates using feed-forward neural network coupled with hybrid particle swarm optimization and gravitational search algorithm. J. Zhejiang Univ. Sci. A 22, 467–480. https://doi.org/10.1631/jzus.A2000316

Ho, L.V., Nguyen, D.H., Mousavi, M., De Roeck, G., Bui-Tien, T., Gandomi, A.H., Wahab, M.A., 2021b. A hybrid computational intelligence approach for structural damage detection using marine predator algorithm and feedforward neural networks. Computers & Structures 252, 106568. https://doi.org/10.1016/j.compstruc.2021.106568

Ho Viet, L., Trinh Thi, T., Ho Xuan, B., 2022. Swarm intelligence-based technique to enhance performance of ANN in structural damage detection. Transport and Communications Science Journal 73, 1–15. https://doi.org/10.47869/tcsj.73.1.1

Hoàng Việt, H., Đỗ Anh, T., Phạm Đức, T., 2023. Utilizing artificial neural networks to anticipate early-age thermal parameters in concrete piers. Transport and Communications Science Journal 74, 445–455. https://doi.org/10.47869/tcsj.74.4.5

Jahangiri, V., Mirab, H., Fathi, R., Ettefagh, M.M., 2016. Tlp structural health monitoring based on vibration signal of energy harvesting system. Latin American Journal of Solids and Structures 13, 897–915.

Kang, F., Li, J., Xu, Q., 2012. Damage detection based on improved particle swarm optimization using vibration data. Applied Soft Computing 12, 2329–2335. https://doi.org/10.1016/j.asoc.2012.03.050

Liu, X., Yi, H., Ni, Z., 2013. Application of ant colony optimization algorithm in process planning optimization. J Intell Manuf 24, 1–13. https://doi.org/10.1007/s10845-010-0407-2

Marques, D., Flor, F., Medeiros, R., Jr, C.P., Tita, V., 2018. Structural health monitoring of sandwich structures based on dynamic analysis. Latin American Journal of Solids and Structures 1–22.

Mirjalili, S., Mirjalili, S.M., Lewis, A., 2014. Grey Wolf Optimizer. Advances in Engineering Software 69, 46–61. https://doi.org/10.1016/j.advengsoft.2013.12.007

Ngoc Long Nguyen, Huu Q.N., Ngoc Lan Nguyen, Tran H.N., 2023. Performance evaluation of the artificial hummingbird algorithm in the problem of structural damage identification. Transport and Communications Science Journal 74, 413–427. https://doi.org/10.47869/tcsj.74.4.3

Ngoc-Nguyen, L., Khatir, S., Nguyen, H.-Q., Nguyen-Tran, H., Bui-Ngoc, D., Wahab, M.A., Bui-Tien, T., 2023. Application of Slime Mould Optimization Algorithm on Structural Damage Identification of Suspension Footbridge, in: Rao, R.V., Khatir, S., Cuong-Le, T. (Eds.), Recent Advances in Structural Health Monitoring and Engineering Structures, Lecture Notes in Mechanical Engineering. Springer Nature, Singapore, pp. 405–415. https://doi.org/10.1007/978-981-19-4835-0_35

Ngoc-Nguyen, L., Ngoc-Tran, H., Khatir, S., Le-Xuan, T., Huu-Nguyen, Q., De Roeck, G., Bui-Tien, T., Abdel Wahab, M., 2022. Damage assessment of suspension footbridge using vibration measurement data combined with a hybrid bee-genetic algorithm. Sci Rep 12, 20143. https://doi.org/10.1038/s41598-022-24445-6

Nguyen-Ngoc, L., Tran-Ngoc, H., Bui-Tien, T., Mai-Duc, A., Wahab, M.A., Nguyen, H.X., Roeck, G.D., 2021. Damage detection in structures using Particle Swarm Optimization combined with Artificial Neural Network. Smart Structures and Systems 28, 1–12. https://doi.org/10.12989/SSS.2021.28.1.001

Rajenderan, R., Jayaguru, C., 2022. Damage Evaluation of Reinforced Concrete structures at lap splices of tensional steel bars using Bonded Piezoelectric Transducers. Latin American Journal of Solids and Structures 19, 1-15. e443. https://doi.org/10.1590/1679-78257069

Sabar, N.R., Ayob, M., Kendall, G., Qu, R., 2012. A honey-bee mating optimization algorithm for educational timetabling problems. European Journal of Operational Research 216, 533–543. https://doi.org/10.1016/j.ejor.2011.08.006

Samal, P., Mohapatra, A., Samal, S., 2023. Application of Artificial Rabbits Optimization Algorithm to the Economic Load Dispatch Problem, in: 2023 4th International Conference for Emerging Technology (INCET). Presented at the 2023 4th International Conference for Emerging Technology (INCET), pp. 1–5. https://doi.org/10.1109/INCET57972.2023.10170612

Shahrouzi, M., Sabzi, A.-H., 2018. Damage detection of truss structures by hybrid immune system and teaching–learning-based optimization. Asian J Civ Eng 19, 811–825. https://doi.org/10.1007/s42107-018-0065-9

Su Fen, N., Shokravi, H., Bakhary, N., Padil, K.H., Zainal Abidin, A.R., 2023. Distance Insensitive Concrete Crack Detection with Controlled Blurriness Using a Convolutional Neural Network. Civil Engineering Infrastructures Journal 56, 117–136. https://doi.org/10.22059/ceij.2022.334291.1802

Wang, L., Cao, Q., Zhang, Z., Mirjalili, S., Zhao, W., 2022. Artificial rabbits optimization: A new bio-inspired meta-heuristic algorithm for solving engineering optimization problems. Engineering Applications of Artificial Intelligence 114, 105082. https://doi.org/10.1016/j.engappai.2022.105082

Yıldız, A.R., Yıldız, B.S., Sait, S.M., Bureerat, S., Pholdee, N., 2019. A new hybrid Harris hawks-Nelder-Mead optimization algorithm for solving design and manufacturing problems. Materials Testing 61, 735–743. https://doi.org/10.3139/120.111378

Zhang, L.-Y., Tseng, M.-L., Wang, C.-H., Xiao, C., Fei, T., 2019. Low-carbon cold chain logistics using ribonucleic acid-ant colony optimization algorithm. Journal of Cleaner Production 233, 169–180. https://doi.org/10.1016/j.jclepro.2019.05.306